The 2012 World Congress on
Advances in Civil, Environmental, and Materials Research (ACEM' 12)
Seoul, Korea, August 26-30, 2012

Flutter Dynamics of a Biplane: A Mathematical Model

Jason McVicar[1)], Caroline DeLong[2)] and Stefanie Gutschmidt[3)]

[1), 2), 3)] *Department of Mechanical Engineering, University of Canterbury, Christchurch 8140, New Zealand*
[3)] *stefanie.gutschmidt@canterbury.ac.nz*

ABSTRACT

As the monoplane configuration is dominant in modern aircraft design, a gap exists pertaining to wing flutter of bi and triplanes. Questions regarding the performance of historical biplanes create a need for the stability and safety of these aircraft to be reconsidered. A coupled reduced order model based on Euler-Bernoulli beam assumptions, St Venant's torsion theory and Theodorsen's unsteady thin airfoil theory is derived to capture the dynamic fluid-structure interactions and estimate critical flutter speeds.

The computational analysis reveals parameter domains of hard and soft flutter, which stand in good qualitative agreement to wind tunnel experiments. Furthermore, critical flutter speeds are predicted to occur at intrinsic resonance modes of coupled torsion and bending motion, induced by parametric excitation of the ambient fluid flow.

1. INTRODUCTION

World War One (WWI) was a time when military hardware advanced and developed at an explosive rate. During this time, military aviation grew rapidly. Very early on it became clear that there would be no such thing as a universal aircraft that could meet the growing needs of reconnaissance, bombing raids, liaison, directing artillery fire and, finally, engaging enemy aircraft in the air. It is from this need that aircraft evolved along different pathways. Depending on design constraints dictated by government pressure and engineering availability, some aircraft changed the war, while others were doomed to fail [1].

In particular, certain biplanes of the era, like the Albatros DV and DVa, and the Nieuport 17 [2], experienced an unusual phenomenon, now known as wing flutter. Flutter of the aircraft wing in flight was often devastating. The problem was never solved, and eventually, biplanes were phased out of service to be replaced by the more modern monoplanes. Today, questions over the safety of historically accurate biplane reconstructions create a need for the stability of biplanes to be reconsidered [2].

Classical wing flutter involves the interactions between the bending and twisting of a thin airfoil and the interaction of aerodynamic and inertial loads; the fluid-structure interaction [3-7]. This type of flutter is often referred to as pitch-plunge flutter [3, 4]. The flutter analysis of monoplane structures has been developed considerably and many methods are now available for analysis. As a result, most flutter models resemble the

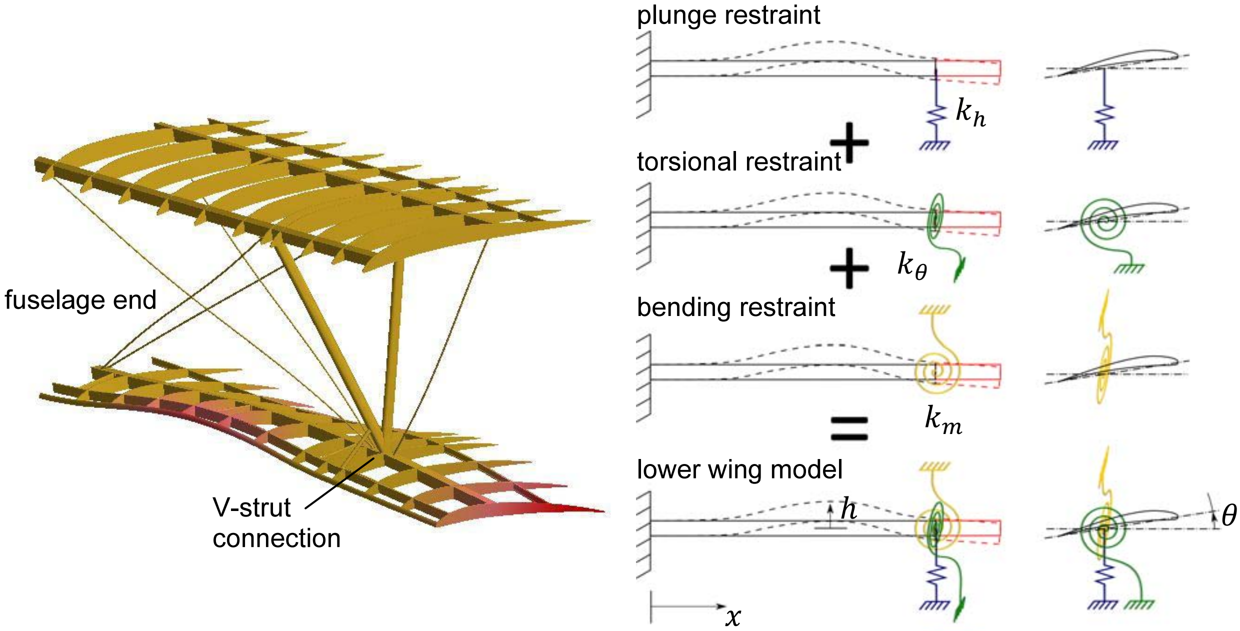

Figure 1: Coupled torsion and bending vibration mode associated to critical flutter speed (left) and schematic sketch of the mathematical model (right) of a V-strut bi-plane structure

cantilever nature of the modern monoplane wing [6]; this was the standard approach for flutter modeling and determination in the 1920's and 1930's, and is the approach set out in "The Wing Flutter Bible" [8]. Methodologies specific to other areas such as biplanes [8, 9] and paper calendars [10-12] have seen significantly less attention. Currently, there exists a knowledge gap specifically in academic literature of biplanes, and the only source that addresses flutter in biplanes was published by Duncan in 1931 [9]. Duncan primarily addresses the flutter of biplane control surfaces, rather than the flutter of wings without control surfaces, which is where flutter was observed in many biplanes and was the likely cause of failure [2].

The following paper presents an analytical model to predict the aeroelastic flutter phenomena occurring in the lower wing of a biplane structure and determine the critical flutter speed.

2. THE REDUCED-ORDER MODEL

The geometry of a biplane is complex and certain structural details do not contribute significantly to the general physical behavior of other elements. Historical evidence [1, 2] indicated that flutter was dominantly observed in the lower wing. Similarly, a finite element analysis (FEA) of a V-strut wing structure revealed that the dynamic behavior of the lower wing could be considered separately to the global biplane structure [13]. Thus, the lower wing system with a carefully chosen set of boundary conditions was considered separately from the rest of the aircraft to investigate in the fluid-structure interactions that would lead to flutter instability. Throughout the investigation, focus was placed on the V-strut design rather than the N- or H-type, as there are no records or documentation to show that these types of biplane ever experienced a flutter problem.

The lower wing was modeled using Euler-Bernoulli beam theory coupled with St Venant's torsion theory. A clamped boundary condition was applied at the fuselage and elastic restraints at the V-strut connection, see Figure 1. Three elastic restraints were used to model the structural interactions with the upper wing at the V-strut connection; the first, a linear spring to model the plunge stiffness, the second, a torsional spring to model the pitch stiffness, and the third a rotational spring to model the stiffness of the "h'-restraint", as detailed in Figure 1. The outboard section of the wing (indicated in red) experiences reduced aerodynamic loading, due to the lift distribution [14], and hence, this section of the wing was neglected in this analysis.

The governing set of equations were derived using Hamilton's principle [15]. The partial differential equations model the mechanical structure (bending and torsion), as well as the aerodynamic forcing of Theodorsen's unsteady thin airfoil theory [7]. In this paper we present the final set of equations, their assumptions as well as a compact analysis. A detailed derivation is documented in DeLong et al. [13] and will be published elsewhere.

The derivation of the governing equations of the lower wing structure with the special set of boundary conditions at the V-strut connection point, closely follows the similar mono-wing derivation in Pierce [7]. The following two partial differential equations describe the bending (1a) and torsional (1b) motion of the lower wing structure [7].

$$\rho A\left(\ddot{h} + b x_\theta \ddot{\theta}\right) + EIh^{IV} = -L, \tag{1a}$$

$$\rho\left(A b x_\theta \ddot{h} + I_P \ddot{\theta}\right) - GJ\theta'' = M_{\frac{1}{4}} + b\left(\frac{1}{2} + a\right)L\ , \tag{1b}$$

with the pitching moment

$$M_{\frac{1}{4}} = -\pi\rho_\infty b^3\left[\frac{1}{2}\ddot{h} + U\dot{\theta} + b\left(\frac{1}{8} - \frac{a}{2}\right)\ddot{\theta}\right]$$

and the aerodynamic lift force

$$L = \pi\rho_\infty b^2\left(\ddot{h} + U\dot{\theta} - ba\ddot{\theta}\right) + a_w\rho_\infty Ub\, C(k)\left[\dot{h} + U\theta + b\left(\frac{1}{2} - a\right)\dot{\theta}\right].$$

Variables and parameters of (1) are identified and listed in Table 1. In this first analysis, structural damping (the damping which exists internally in the wing structure) has been neglected in order to separately analyze the dissipative term that originates from the fluid-structure interaction. The left-hand sides of (1) contain the system response, while the right-hand sides model the aerodynamic forcing. Theodorsen's lift equations and a strip theory model were employed [7]. It should be noted that strip theory models neglect any 3D effects. The function $C(k)$ of the lift force refers to the Theodorsen Function which models the reduction in lift and phase lag as a function of reduced frequency, $k = b\omega/U$.

Table 1: List of Variables and Parameters (for detailed descriptions see [7])

	Variables:
h	plunge degree of freedom
θ	pitch degree of freedom
	Parameters:
ρA	wing mass per unit length
ρI_P	rotational inertia per unit length about neutral line
b	semi-chord length
e	dimensionless description of the center of mass location
a	dimensionless description of the flexural axis
x_θ	static unbalance parameter ($x_\theta = e - a$)
GJ	torsional stiffness
EI	bending stiffness
k_h	effective plunge stiffness at V-strut attachment
k_θ	effective torsional stiffness at V-strut attachment
k_m	effective bending stiffness at V-strut attachment
a_w	lift curve slope of the wing
U	air speed
ρ_∞	air density

The associated boundary conditions to the coupled fluid-mechanics wing structure are:

clamped (fuselage) end: V-strut connection point:

$$h(0,t) = 0 \qquad EIh''(L,t) + k_m h'(L,t) = 0$$
$$h'(0,t) = 0 \qquad k_h h(L,t) - EIh'''(L,t) = 0 \qquad (2)$$
$$\theta(0,t) = 0 \qquad k_t \theta(L,t) - GJ\theta'(L,t) = 0$$

Note, that all restraints applied at the V-strut are implemented into the system through the boundary conditions at the same location. A $(\dot{\ldots})$ in Eq. (1) indicates a time derivative, a $(\ldots)'$ and a superscript roman numeral indicate a derivative with respect to x of the given order, respectively.

The model was used to predict the behaviour of an XPS foam wing that was designed and built for wind tunnel tests [13]. The wing parameters for the model were approximated by various methods. The mass per unit length, inertia per unit length, semi-chord length and center of mass of the XPS foam wing were measured. The flexural axis, torsional stiffness, bending stiffness and the three restraint stiffness values (k_h, k_θ, k_m) were approximated using FEA [13].

3. FORCED VIBRATIONS OF COUPLED SYSTEM

Equations (1) and (2) are solved by applying separation of variables to separate the time-dependent amplitudes from the space variables. The uncoupled system in (1) is used to obtain the mode shapes, which are used in the Galerkin method to solve the forced vibrations of the system. The flexible mode shapes are calculated over the inboard section of the wing only.

Applying Galerkin's method, considering the first bending and the first torsional modes and letting $h(x,t) = q_{11}(t)H_1(x)$ and $\theta = q_{12}(t)\Theta(x)$ yields the following set of ordinary differential equations:

$$\begin{bmatrix} m_1 J_{111} & I_1 J_{112} \\ m_2 J_{112} & I_2 J_{211} \end{bmatrix} \begin{bmatrix} \ddot{q}_{11} \\ \ddot{q}_{21} \end{bmatrix} + U \begin{bmatrix} c_1 J_{111} & c_2 J_{112} \\ c_3 J_{112} & c_4 J_{211} \end{bmatrix} \begin{bmatrix} \dot{q}_{11} \\ \dot{q}_{21} \end{bmatrix} + \begin{bmatrix} EI\, J_{113} & U^2 k_1 J_{112} \\ 0 & U^2 k_2 J_{211} - GJ\, J_{213} \end{bmatrix} \begin{bmatrix} q_{11} \\ q_{21} \end{bmatrix} = \mathbf{0},$$

$$\boldsymbol{M}\ddot{\boldsymbol{q}} + U\boldsymbol{C}\dot{\boldsymbol{q}} + \boldsymbol{K}\boldsymbol{q} = \mathbf{0}, \tag{3}$$

with the integration constants being defined as:

$$J_{211} = \int_0^L \Theta_1 \Theta_1 dx\,; \quad J_{212} = J_{112} = \int_0^L H_1 \Theta_1 dx\,; \quad J_{213} = \int_0^L \Theta_1 \Theta_1^{''} dx$$

$$J_{111} = \int_0^L H_1 H_1 dx\,; \quad J_{113} = \int_0^L H_1 H_1^{IV} dx$$

and

$$\boldsymbol{m_1} = \boldsymbol{\rho A} + \boldsymbol{\pi \rho_\infty b^2},$$
$$\boldsymbol{m_2} = \boldsymbol{\rho} Abx_\theta + \frac{1}{2}\pi\rho_\infty b^3 - \boldsymbol{b^3}\pi\rho_\infty \left(\frac{\mathbf{1}}{\mathbf{2}} + \boldsymbol{a}\right),$$
$$\boldsymbol{I_1} = (\boldsymbol{\rho Abx_\theta} - \boldsymbol{\pi\rho_\infty b^3 a}),$$
$$\boldsymbol{I_2} = \rho I_P + \boldsymbol{\pi\rho_\infty b^4}\left(\frac{\mathbf{1}}{\mathbf{8}} - \frac{\boldsymbol{a}}{\mathbf{2}}\right) + \left(\frac{\mathbf{1}}{\mathbf{2}} + \boldsymbol{a}\right)\pi\rho_\infty b^4 a,$$
$$\boldsymbol{c_1} = a_w \rho_\infty b\,,$$
$$\boldsymbol{c_2} = \boldsymbol{a_w \rho_\infty b^2}(\mathbf{1} - \boldsymbol{a}),$$
$$\boldsymbol{c_3} = -\boldsymbol{a_w \rho_\infty b^2}\left(\frac{\mathbf{1}}{\mathbf{2}} + \boldsymbol{a}\right),$$
$$c_4 = \boldsymbol{\pi\rho_\infty b^3} - \pi\rho_\infty b^3\left(\frac{\mathbf{1}}{\mathbf{2}} + \boldsymbol{a}\right) - a_w\rho_\infty \boldsymbol{b^3 C(k)}\left(\frac{\mathbf{1}}{\mathbf{2}} + \boldsymbol{a}\right)\left(\frac{\mathbf{1}}{\mathbf{2}} - \boldsymbol{a}\right),$$
$$\boldsymbol{k_1} = \boldsymbol{a_w \rho_\infty b},$$
$$\boldsymbol{k_2} = -\boldsymbol{a_w \rho_\infty b^2}\left(\frac{\mathbf{1}}{\mathbf{2}} + \boldsymbol{a}\right).$$

4. ANALYSIS

Using the estimated wing parameters [13], the governing equations were solved over a range of air speeds. From this, modal frequency and damping curves were produced which are shown in Figure 2. The modal frequency plot indicates the interactions that exist between modes, while the damping plot predicts the stability of the system. For positive values of the modal damping parameter the wing, undergoing small disturbances, will oscillate about a stable equilibrium position. Conversely, if the damping is negative, the aerodynamic loading will force the wing away from its steady position following a disturbance; this is where the flutter instability will occur.

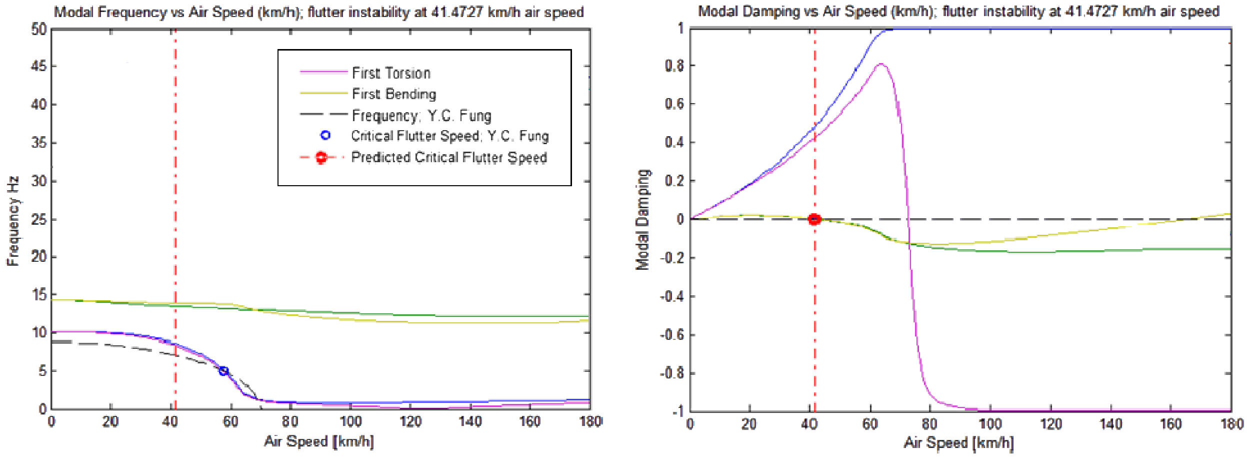

Figure 2: Modal frequency and damping plots for estimated parameters

For comparison, we plotted the flutter speed predicted by the methodology set out by Y. C. Fung [6] (indicated by the dashed line and blue circle in Figures 2 and 3). This is a simpler analysis considering the quasi steady state aerodynamic loading. This method also considers first bending and torsion modes, and typically provides a conservative estimate. It can be seen that the obtained results are of similar order to this simple but established method.

The first bending mode is predicted to become unstable at an air speed of 41 km/h. At this air speed instability was not observed in wind tunnel tests, but a region of very low damping was observed for speeds between 61 km/h and 70 km/h. Over this region, small disturbances in the flow resulted in oscillation of the wing in pitch and plunge of near constant amplitude; indicating that the system was very near a region of instability (flutter). As the air speed was increased, the system appeared to become more stable, this is reflected in the damping plot as the damping of the unstable bending mode trends back toward zero.

Final failure of the wing was observed at 91 km/h, this is somewhat above the predicted instability of the first torsion mode at 73 km/h. This discrepancy could stem from any of the following reasons:

- Experimental errors in determining the wing parameters.
- Increase in effective torsional stiffness of the wing under increased wind loads due to bending deformations. Increasing the torsional stiffness parameter (GJ) from 1 to 1.5 causes the first flutter speed to increase from 41 km/h to 56 km/h, and the second flutter speed to increase from 73 km/h to 89 km/h. These values are in close agreement with the observed flutter events, but do not fully validate the model. The resulting damping and frequency plots are shown in Figure 3.
- Neglecting of structural damping in the reduced order model. The experimental wing was of XPS foam construction and has high structural damping.

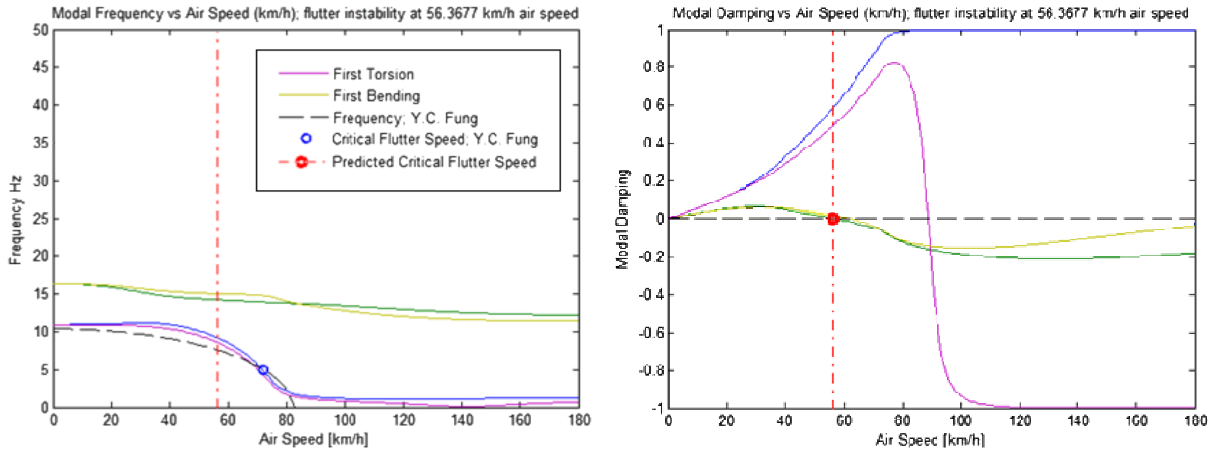

Figure 3: Modal frequency and damping plots for the revised torsional stiffness (GJ)

The negative damping observed in the first bending mode indicates that divergent flutter should have been observed at 41 km/h. However, the model does not include the structural damping due to the deformation of the wing structure. The experimental wing which was used for the wind tunnel testing [13] was of foam construction; a material with typically high damping coefficients. If the additional damping was included in the model, the modal damping curves would be shifted further toward the stable region. This observation provides strong evidence to suggest that the model has captured the variance in dynamics of the system for varying air speeds.

The Galerkin method was performed considering only the uncoupled vibration modes of the wing structure. However, the finite element analysis showed that there were distinct vibration modes which were neither purely torsion nor bending, but rather a coupled vibration mode shape. As these coupled mode shapes are not accounted for in the current ROM, their behavior with varying airspeed, and ultimately their stability, have not been considered. In future investigations a plate theory approach would be more suitable, as a 2D mode shape representation would allow for coupled bending and torsional modes.

As the slope of the damping curve for the first torsional mode near the critical flutter speed is steep (Figures 2 and 3) a *hard flutter* instability is predicted. *Hard flutter* occurs where the damping of the system changes from large positive to large negative damping over a small range of airspeed. This is undesirable in a system as it leads to a sudden change from highly stable to highly unstable with very little warning which can be disastrous for a pilot in the case of aviation. Conversely, *soft flutter* is an instability where the damping transitions gradually from positive to negative damping values. During *soft flutter* the wing will oscillate while the system remains stable, allowing for enough reaction time to change the operating conditions (such as airspeed for an aircraft), preventing failure. Both hard and soft flutter are observed in the modal damping plots. The instability of the first torsion mode is clearly a hard flutter event with a very sudden onset, while the instability of the first bending mode follows a very gradual transition from stable to unstable. Soft flutter behavior was observed during wind tunnel testing; as characterized by the prolonged period of borderline stability between 61 km/h and 70 km/h wind speeds.

SUMMARY AND CONCLUSION

This work presents a first analytical approach to predict critical flutter speeds of a biplane wing structure. Speeds were calculated based on estimated parameters and uncoupled mode shapes. The results stand in good qualitative agreement with data obtained from both FEA and wind tunnel testing of a foam wing structure [13]. Although the results stand in good qualitative agreement with the performed wind tunnel tests, the proposed mathematical model is limited by its simplistic nature. It was observed that critical flutter speeds were highly sensitive to input parameters and mode shapes. Due to the simple beam model and the applied Euler-Bernoulli and St Venant's torsion theory assumptions, the mode shape functions of bending and torsion are implemented separately (uncoupled). Our analytical investigations, in parallel to the finite element analysis, revealed that a plate theory approach would be more suitable, especially to achieve quantitative agreements with wind tunnel results.

ACKNOWLEDGEMENTS

This work was performed within the framework of the Final Year Projects of the BE(Hons) program at the University of Canterbury. We gratefully acknowledge the works of finite element modelling and wind tunnel testing by the other team members, Daniel Mossman and Samuel Hamilton, who validated the analytical results and will be published elsewhere.

REFERENCES

1. VanWyngarden, G., *Albatros Aces of World War One: Part 2.* 2007, Oxford: Osprey Publishing.
2. Mikesh, R.C., *Albatros DVa: German Fighter of World War 1 (Famous Aircraft of the National Air and Space Museum)* 1980: Smithsonian.
3. Abbas, L.K., et al., *Numerical studies of a non-linear aeroelastic system with plunging and pitching freeplays in supersonic/hypersonic regimes.* Aerospace Science and Technology, 2007. **11**(5): p. 405-418.
4. Bisplinghoff, R.L., H. Ashley, and R.L. Halfman, *Aeroelasticity*. Addison-Wesley series in mechanics1955, Cambridge, Mass.,: Addison-Wesley Pub. Co. 860 p.
5. Fazelzadeh, S.A. and A. Mazidi, *Nonlinear Aeroelastic Analysis of Bending-Torsion Wings Subjected to a Transverse Follower Force.* Journal of Computational and Nonlinear Dynamics, 2011. **6**(3).
6. Fung, Y.C., *An Introduction to the Theory of Aeroelesticity.* 2002, United States Dover Publications
7. Pierce, D.H., *Introduction to Structural Dynamics and Aeroelasticity* 2004, United Kingdom Cambridge University Press.
8. Duncan, R.F., *The Flutter of Aeroplane Wings.* 1929, London: His Majesty's Stationery Office
9. Duncan, R.F., *Flutter of Monoplanes, Biplanes and Tail Units*1931, London: His Majesty's Stationery Office
10. G. Spelsberg-Korspeter, D.H., P. Hagedorn, *Self-Excitation Mechanisms in Paper Calenders Formulated as a Stability Problem.* TECHNISCHE MECHANIK, 2011. **31**(1): p. 15 – 24.

11. Spelsberg-Korspeter, G., *Structural optimization for the avoidance of self-excited vibrations based on analytical models.* Journal of Sound and Vibration, 2010. **329**(23): p. 4829-4840.
12. Wiendl, S.S.-K., G.; Hagedorn, P. *A Dynamical Model of a Paper Calendering Unit with Surface Wear*. in *COMPDYN 2011 3rd International Conference on Computational Methods in Structural Dynamics and earthquake Engineering*. 2011. Corfu, Greece.
13. DeLong, C.a.H., Samuel, and McVicar, Jason and Mossman, Daniel, *Aerodynamic Forensic Engineering Investigation: Wing Flutter Associated with the Albatros DVa*, 2011, University of Canterbury: Christchurch, New Zealand. p. 1-27.
14. White, F.M., *Fluid Mechanics*. 5 ed2003, New York: McGraw Hill.
15. Rixen, M.G., *Mechanical Vibrations Theory and Application to Structural Dynamics.* 1996, London: John Wiley and Sons